In MICCAI 2003 proceedings
LNCS 2879: 9-15

# Tissue-Based Affine Registration of Brain Images to form a Vascular Density Atlas

Derek Cool, Dini Chillet, Jisung Kim, Jean-Phillipe Guyon, Mark Foskey, and Stephen Aylward

Computer Aided Display and Diagnosis Laboratory
Department of Radiology, The University of North Carolina at Chapel Hill, USA
{cool, aylward}@unc.edu
http://www.caddlab.rad.unc.edu

**Abstract.** Anatomic tissue atlases of the brain are widely used within the medical world and are important for identifying tissue and structural aberrations and inconsistencies within an individual. Unfortunately, there are many procedures and diseases that require examination of the brain's vascular system, which is not easily identifiable in anatomic atlases. We present a new concept of a brain vascular atlas, formed through tissue-based registration, to capture expected vascular characteristics and their variance. This vascular atlas can be used to assess the vascular variations within an individual and aid in diagnostics and pre-surgical planning. In this paper, a vascular density atlas is formed and demonstrated for use in detecting and localizing vascular anomalies.

## 1 Introduction

Creation of an average 3-dimensional standardized brain and modeling its common variations is important both clinically and in research. An atlas of the brain establishes a generalized societal form and has multiple benefits, including use as a statistical prior for effective assessment of aberrations within individuals. Numerous types of anatomical atlases have been formed. These atlases are effective tools for tissue-based analysis; however, they fail to illustrate the cardiovascular network of the brain.

Generation of a tool to assess cranial vascular distribution would have both clinical and research applications. Medical applications include pre-operative planning and diagnosis, identification of vascular anomalies, and assessment of an individual's vascular changes over time. Such a tool might also aid in diagnosis of mental disorders, such as schizophrenia, that have a strong genetic component; embryological research suggests that the formation of the cranial vascular system precedes tissue development and potentially drives its structural formation [7], making it a possible determinant of cranial anatomy and a possibly more direct measure of the genetic component of such mental disorders. An atlas of vasculature could also be advantageous for stroke assessment– identifying affected areas, analyzing vascular malformation, and estimating arterial

compensation. Finally, a vascular atlas could be used in conjunction with an anatomical atlas for additional verification and statistical validation.

This paper proposes the formation of a vascular atlas as a valid and effective tool for measuring expected cerebral vessel distribution and illustrates its accuracy in estimating a societal average and variations. Forming the average vascular matrix within brain matter might not only be useful for identifying subtle changes in vessel formation not visible through standard tissue analysis, but it may also effectively imply tissue abnormalities through underlying vascular irregularity. Construction of the proposed vascular atlas involves tissue-based anatomical registration of density maps for an individual's cranial vessels, resulting in a mean vascular density atlas with expected variance. This approach is advantageous for the parallel formation of accurate, correlated anatomic and vascular atlases for tissue-based analysis.

## 2 Methods

Various registration techniques could be used for vascular atlas formation. We present a solution built on a tissue-based correlation of individual brains using mutual-information registration [1, 6] applied through affine transformations. Transforms from tissue alignment are then applied to corresponding vessel density maps to form a vascular mean with expected variance. Our atlas registration technique varies from the vessel-to-image vascular atlas formed by Chillet [3], as our approach focuses on the creation of a mean vascular brain resulting from tissue alignment rather than vessel registration.

Atlas formation requires a set of brain normals containing mutually aligned T2 MRIs and Magnetic Resonance Angiograms (MRA). For our experiment, a rigid body transformation of individuals' T2 images onto their corresponding MRAs ensured proper correlation between the two images [5]. Since both scans were acquired in one sitting, it is reasonable to expect negligible brain distortion between the images.

### 2.1 Vessel Extraction

Formation of the vascular density map requires extraction of all arterial vessels visible within a subject's MRA. For our vessel segmentation solution we utilize a centerline traversal [2] approach. This method executes a multi-scale traversal of a vessel's centerline, initiated from a point found on or near the tube. The radius of the vessel is then estimated using that centerline [8, 9].

During vessel modeling, only cerebral arteries, not veins, were gathered. This was done to improve the standardization of the vessel trees, since the image intensity of arterial vessels was more consistent across subjects' MRAs, when compared to veins. It is acknowledged that visual extraction of arteries is not exhaustive nor guaranteed to draw all available vessels; however, with meticulous segmentation attention and averaging of multiple vascular trees, such limitations fall within a reasonable range of uncertainty. Clean MRA scans are essential for proper vascular tree collection.

### 2.2 Formation of Density Map Images

After vascular tree segmentation, the Danielsson distance algorithm (DD) [4] is applied to the vessels, to generate a Euclidean distance field. The DD algorithm systematically generates an image for which each voxel contains the Euclidean distance to the nearest vessel. The distance maps represent vascular density images, by identifying probabilistic vessel locations as opposed to absolute binary vessel definitions. This approach forms clouds of expected vascular existence, which when combined with other density maps generates the average expected vascular density for a normal brain.

### 2.3 Atlas Registration and Generation

The vascular atlas is formed using tissue-based mutual-information registration [1]. Using Parzen windows for estimating probability density distributions, the mutual-information applies an affine transform to the T2 weighted image to align it with the atlas template. Initially, each T2 brain image is registered to a single brain that is used as the atlas template. An anatomical atlas is formed through summation of the registered images to form a mean. This procedure is repeated using the newly formed atlas as the atlas template in order to remove bias toward the originally template individual. Repetition of this cycle gradually moves toward an unbiased, general atlas. After satisfactory formation of a general atlas, the affine transformations from the tissue registration are applied to their corresponding vascular density map to align each field properly in the anatomical match. Combining the aligned fields forms the vascular mean and expected variance.

### 2.4 Assessment and Evaluation

To assess the validity of the vascular atlas for estimating intra-cranial vasculature, we compare individuals' distance fields with the vascular atlas using voxel-by-voxel scoring. Evaluating on a per voxel basis allows regions of statistical deviation within an individual's distance field to be localized. These scores are then used to quantify global differences through the subjects.

To form the standard distribution, we use z-score analysis to estimate an individual's adherence to the atlas. Z-score is calculated using the following formula:

$$z_v = \frac{\chi_v - \mu_v}{\sigma_v}$$

where $\chi_v$ represents an individual's brain intensity at location v, $\mu_v$ represents the mean atlas intensity for that location, and $\sigma_v$ represents the standard deviation for that voxel.

A large z-score value indicates a statistical anomaly at that voxel for an individual. Gaussian distributed populations can be assessed based on the z-score distribution within and across individuals. Computed for each individual, this process allows identification of outliers with subtle vascular variation.

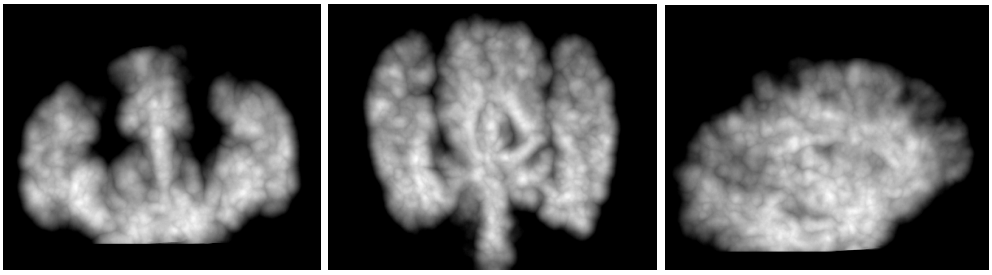

**Fig. 1.** Images of vascular density atlas (From Left): coronal, axial, sagittal views

## 3 Results

Figure 1 illustrates coronal, axial and sagittal maximum intensity projections of the vascular density atlas formed through tissue-based registration of nine subjects. The vascular cloud segments for the left and right hemispheres and medial arteries are clearly defined and distinct. Cranial shape is evident and locations of large structures, such as ventricles, are implied within the vascular spaces.

Table 1 shows the z-score results indicating the percentage of an individual's voxels that deviate from the *vascular atlas*. Table 2 shows percent deviation from the *anatomical atlas*. The statistical expectation for normal distribution is indicated as well in both measures. Most subjects' vascular maps fall within the expected normalized deviation the atlas. Two vascular outliers, subjects 09 and 04, illustrate the atlas capability of identifying subtle changes in vasculature and are illustrated in Fig. 2 where deviation images highlighting deviant areas are compared with conforming subjects 05 and 08.

**Table 1.** Percentage of voxels having z-scores contained within select standard deviations of mean *vascular density atlas*.

| | **Standard Deviations** | | | | | |
|---|---|---|---|---|---|---|
| **Subject** | **0.2** | **0.6** | **1.0** | **1.4** | **1.6** | **2.0** |
| 01 | 15.10 | 44.10 | 68.48 | 85.54 | 91.04 | 97.42 |
| 02 | 15.49 | 44.78 | 69.16 | 86.67 | 92.30 | 98.36 |
| 03 | 15.60 | 46.32 | 73.17 | 89.80 | 94.42 | 98.80 |
| **04** | **13.03** | **38.49** | **62.06** | **80.62** | **87.37** | **96.35** |
| 05 | 16.19 | 47.45 | 73.60 | 90.54 | 94.99 | 99.17 |
| 06 | 16.41 | 47.43 | 73.03 | 89.87 | 94.71 | 98.99 |
| 07 | 15.26 | 44.49 | 69.72 | 87.41 | 92.82 | 98.35 |
| 08 | 15.56 | 45.58 | 71.11 | 88.43 | 93.30 | 98.55 |
| **09** | **11.48** | **33.60** | **54.38** | **72.50** | **80.26** | **92.11** |
| **Normal Dist** | 15.9 | 45 | 68 | 84 | 89 | 95.4 |

**Table 2.** Percentage of voxels having z-scores contained within select standard deviations of *mean anatomical atlas*.

| | Standard Deviations | | | | | |
|---|---|---|---|---|---|---|
| **Subject** | **0.2** | **0.6** | **1.0** | **1.4** | **1.6** | **2.0** |
| 01 | 12.92 | 47.96 | 76.76 | 90.18 | 93.50 | 97.26 |
| 02 | 13.04 | 45.97 | 71.88 | 85.21 | 89.11 | 94.34 |
| 03 | 14.98 | 48.53 | 69.95 | 81.74 | 86.12 | 93.03 |
| **04** | **10.65** | **39.69** | **67.70** | 85.42 | 90.24 | 95.69 |
| 05 | 16.21 | 53.12 | 75.46 | 86.99 | 90.84 | 95.93 |
| 06 | 13.14 | 48.04 | 74.35 | 86.87 | 90.52 | 95.48 |
| 07 | 11.93 | 45.13 | 75.83 | 90.85 | 94.23 | 97.70 |
| 08 | 12.22 | 45.06 | 72.82 | 86.64 | 90.55 | 95.58 |
| 09 | 11.93 | 44.68 | 73.74 | 89.43 | 93.24 | 97.22 |
| **Normal Dist** | 15.9 | 45 | 68 | 84 | 89 | 95.4 |

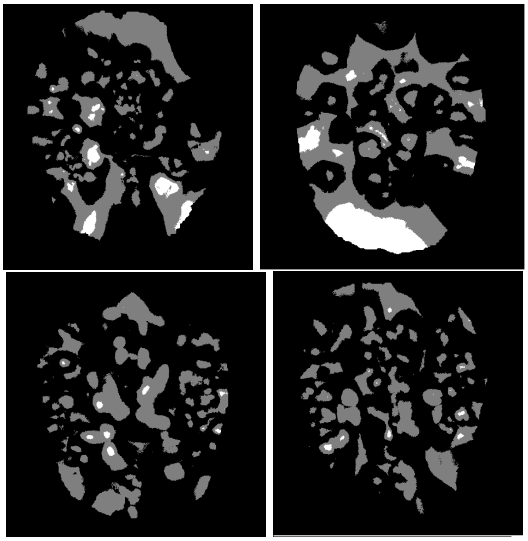

**Fig. 2.** Images of vascular density Z-score distributions (black = 0-0.9, gray = 1-1.9, white > 2) (Top Row): Deviatant individuals- 04 (left) and 09 (right) (Bottom Row): Conforming individuals- 05 (left) and 08 (right)

## 4 Discussion

The generated vascular density atlas showed tight formation and distinct brain segments representing different lobe vasculature. While the vascular branches formed clouds of probable density as opposed to distinct vessels, the major branches and vascular structures, such as the Circle of Willis, were clearly visible within the atlas. Additionally, structural anatomic silhouettes of the skull, ventricles, and spinal base were visible within the vascular atlas, which was to be expected as the atlas was formed through tissue registration. Qualitative results indicate a reasonable alignment of tissue and vascular tubes for formation of parallel creation. Quantitative validation of the vascular atlas through individual comparisons showed a normal deviation distribution for most subjects. Z-score analysis illustrated a largely normalized fit of subject vessels to the atlas. The deviation of individual vascular images from the calculated mean fell within a normalized distribution fit outside of 0.4 deviations. Inside of 0.4 deviations, the accuracy fell slightly below a normalized distribution, which can be expected since the atlas registration is tissue-based, as opposed to vascular. It is interesting to note, however, that in almost all cases the vascular atlas had greater percentages within 0.2 deviations than the tissue atlas. This is largely due to higher contrast within tissue images, as opposed to the gentle gradient slopes formed in a Euclidean distance field.

Vascular outliers were present and indicate subtle arterial variations from the general population. Z-score analysis of subject 09 showed heavy vascular deviation in the anterior lobe of the brain and further examination of the subject's vascular tree verified that anterior vessel formation was less pronounced within the individual. While other factors such as diminished arterial flow during the MRA scan could conceivably have caused this anomaly, the arterial prominence in other vessels of the scan support the integrity of the scan. Regardless, the result illustrates the atlas' ability to identify incongruent vasculature otherwise not visibly apparent. Anatomical analyses indicated no significant variation of subject 09 from the tissue atlas; suggesting either a complete lack of physical manifestations of the vascular anomaly within the tissue, or more likely that such tissue deviations are not easily identifiable through tissue comparison. This further suggests the atlas' analytical potential for identification of cranial diseases and abnormalities.

Subject 04 also demonstrated vasodeviation, this time coupled with anatomic irregularity. A slight physical deformation in subject 04's visual anatomy was apparent in anatomic deviation around the anterior brain. Heavy vascular deviation in the vicinity of the aberration identified a manifested vascular shift, due to the physical abnormality. It is also important to note that localized vascular deviation was evident within the visual cortex and other parts of the occipital lobe, supporting the possibility of modifications in the visual sensory processing region of the cortex which would be expected given the subjects physical abnormality.

Our experiment, while not conclusive, suggests formation a brain vascular atlas as a valid tool for estimating a societal norm. Conclusive results will require

collection of additional subjects to form a tighter fitting atlas representative of a larger portion of society. Regardless, the results of our study indicate a correlation between the brain's vasculature and tissue composition. Our limited subject-to-atlas comparisons not only accurately identified abnormal individuals, but also highlighted potential diagnostic advantages of a vascular atlas.

Development software was built using the NLM's Insight toolkit. This work was supported by the following grants: NIH/HLB R01 HL69808, Whitaker Foundation RG010341, and NLM N01 LM03501. Additional details and illustrations are available on our website, http://caddlab.rad.unc.edu.

## References

1. Viola P, Wells III W. "Alignment by Maximization of Mutual Information", International Journal of Computer Vision, 1997, 24(2):137-154
2. Aylward SR. "Vascular Image Registration for Intra-Operative 3D Ultrasound Annotation", International Journal of Computer Vision, March 2003, pages 15
3. Chillet D, Jomer J, Cool D, Aylward SR. "Vascular Atlas Formation Using a Vessel-to-Image Affine Registration Method", MICCAI 2003, March 2003, Pages 8
4. Danielsson PE. "Euclidean Distance Mapping", Computer Graphics and Image Processing, 14, 1980, pp. 227-248
5. Guyon JP, Foskey M, Kim J, Firat Z, David B, Aylward SR. "VETOT, Volume Estimation and Tracking Over Time: Framework and Validation", MICCAI 2003, March 2003, Pages 8
6. Hill D. Medical Image Registration. 2000
7. Seydel C. "Organs Await Blood Vessels' Go Signal" Science, 2001, 291:2365
8. Aylward SR, Bullitt E, Pizer SM, Eberly D, "Intensity ridge and widths for tubular object segmentation and registration", IEEE Workshop on Mathematical Methods in Biomedical Image Analysis, 1996, 131-138
9. Aylward SR, Bullitt E, "A Comparison of Methods for Tubular-Object Centerline Extraction", IEEE Transactions on Medical Imaging, 21(2), 2002, pp. 61-76